

Charge carrier mobility in a two-phase disordered organic system in the low-carrier concentration regime

Cristiano F. Woellner,^{1,*} Zi Li,² José A. Freire,³ Gang Lu,² and Thuc-Quyen Nguyen¹

¹*Department of Chemistry and Biochemistry, University of California, Santa Barbara, California 93106, USA*

²*Department of Physics and Astronomy, California State University Northridge, California 91330, USA*

³*Departamento de Física, Universidade Federal do Paraná, 81531-990, Curitiba-PR, Brazil*

(Received 25 June 2013; published 30 September 2013)

In this paper we use a three-dimensional Pauli master equation to investigate the charge carrier mobility of a two-phase system which can mimic donor-acceptor and amorphous-crystalline bulk heterojunctions. By taking the energetic disorder of each phase, their energy offset, and domain morphology into consideration, we show that the carrier mobility can have a completely different behavior when compared to a one-phase system. When the energy offset is equal to zero, the mobility is controlled by the more disordered phase. When the energy offset is nonzero, we show that the mobility electric field dependence switches from negative to positive at a threshold field proportional to the energy offset. Additionally, the influence of morphology, through the domain size and volume ratio parameters, on the transport is investigated and an approximate analytical expression for the zero field mobility is provided.

DOI: [10.1103/PhysRevB.88.125311](https://doi.org/10.1103/PhysRevB.88.125311)

PACS number(s): 72.80.Le, 72.20.Ee, 73.61.Ph

I. INTRODUCTION

High performance conjugated polymers have gained significant interest in recent years due to their low-cost processing and their high ductility, a vital feature for applications in flexible electronics giving them a significant advantage over other technologies based on crystalline semiconductors.¹ Despite their great potential for applications, the performance of devices based on organic materials is still somewhat disappointing. Thus, a better understanding of charge transport in these materials is required.

Phenomenological models describing charge transport in disordered organic materials have a long history that began with Bässler in the early 1980s. In 1981 he proposed a model to describe the charge carrier mobility in time of flight (TOF) experiments² that became a reference in the field. In this model the charge transport was postulated to occur via hopping between localized electronic states and the energy of these states was taken to be Gaussianly distributed. In 1993, Bässler extended his model to take into account the positional disorder. Since then this model has been known as the Gaussian disorder model (GDM).³

Although TOF experiments have proven to be a useful tool for characterizing the electron and hole mobilities in disordered organic materials, this technique does not reproduce the charge densities actually found in typical devices such as organic light-emitting diodes (OLEDs)⁴ and organic field-effect transistors (OFETs).⁵ In the early 2000s, using rigorous theoretical methods, Baranovskii *et al.*,^{6,7} Schmechel,⁸ and others^{9–11} showed the importance of taking into account the carrier density dependence in the GDM. In 2005 Pasveer *et al.*,¹² based on a numerically exact approach proposed a parametrization of the mobility as a function of temperature, electric field, level of disorder, as in the GDM, but with the novelty of including a dependence on the charge carrier density, which proved crucial in characterizing devices based on organic materials.

With the advent of solar cells based on bulk heterojunctions (BHJs)^{13,14} the need for models that describe the charge

transport in such systems aroused. Still in 2005, not motivated by modeling charge transport in blends, Watkins *et al.*¹⁵ proposed an effective model based on the dynamical Monte Carlo method to generate the morphologies of binary mixtures. In this model the electron and hole mobilities were assumed constant. In 2010, using a proper combination of Pasveer and Watkins approaches, Koster showed for the first time that the mobility in donor-acceptor blends could exhibit a negative electric field dependence.¹⁶

Despite these advances, all models so far for charge transport in BHJs explicitly have assumed that the transport occurs exclusively in one phase (donor or acceptor) independent of the difference in energy between the electronic states of the two phases or the applied electric field.^{17,18}

In this paper, we propose a model based on a Pauli master equation that describes the charge transport in a system composed of two distinct phases, each of which consisting of only localized electronic states. The density of states (DOS) of the system is assumed to be a bimodal Gaussian distribution,¹⁹ wherein the width of each mode is associated with the disorder in each phase and the energy offset of the two peaks is related to the energy offset between the transport levels of the two phases. Bimodal Gaussian DOS has also been used to describe organic systems containing transporting sites and traps (see Ref. 20). We consider only single-carrier transport. The morphology of the binary blend is generated from a Monte Carlo simulation in a manner similar to the one used by Watkins. The morphology is completely specified by two parameters: the volume ratio between the two materials, and a characteristic length associated with the interfacial area between the two phases. Finally, after obtaining the system morphology, the stationary solution of the Pauli master equation (obtained numerically) gives the mobility as a function of temperature, applied electric field, and charge density.

The rest of the paper is organized as follows: In Sec. II, we introduce the charge transport model for a two-phase mixture. The effect of disorder and the role of the energy offset between the two phases are addressed in Sec. III. Section IV analyzes

the influence of morphology by varying the parameters associated with domain size (characteristic length) and volume ratio. In Sec. V, the electric field dependence of a two-phase system with equal and different energetic disorder is investigated. The last section contains our conclusions.

II. MODEL

Our approach can be separated in two parts: the morphology generation and the charge transport modeling in the generated blend. The morphology part is based on a lattice-gas model²¹ of a binary mixture developed by Watkins *et al.*¹⁵ The system is defined on a regular cubic lattice of N sites and lattice parameter a . The phase-1 is constituted by αN sites and phase-2 by $(1-\alpha)N$ sites, where α is the volume ratio. $\alpha = \{0, 1\}$ represent the limiting cases of a one-phase system. The lattice is initialized with a random mixture of the constituents with fixed α . To simulate a real two-phase system, such as donor-acceptor or amorphous-crystalline blends, a phase segregation is induced. This is accomplished with a Monte Carlo simulation by adjusting the interaction energy between the constituents. At every Monte Carlo step a pair of neighboring sites is randomly chosen and the total energy of the system before and after the sites swap their positions is calculated. If the total energy decreases the swap is automatically accepted, otherwise a nonzero probability of acceptance is associated with the exchange.

The phase separation is characterized by a characteristic length, known as the domain size, defined by¹⁶

$$b = \frac{6 \min(\alpha, 1 - \alpha) V}{A}, \quad (1)$$

where V is the total volume and A is the interfacial area. The Monte Carlo simulation is performed until the desired domain size is reached. Notice that the morphology is defined by only two parameters, the volume ratio α , and the domain size b . Figure 1 shows a two-dimensional slice of the morphology with an equal amount of constituents ($\alpha = 0.5$). It illustrates the concept of the domain size for two typical cases: a homogeneous mixture ($b = 2$ nm) and a partially phase separated ($b = 6$ nm).

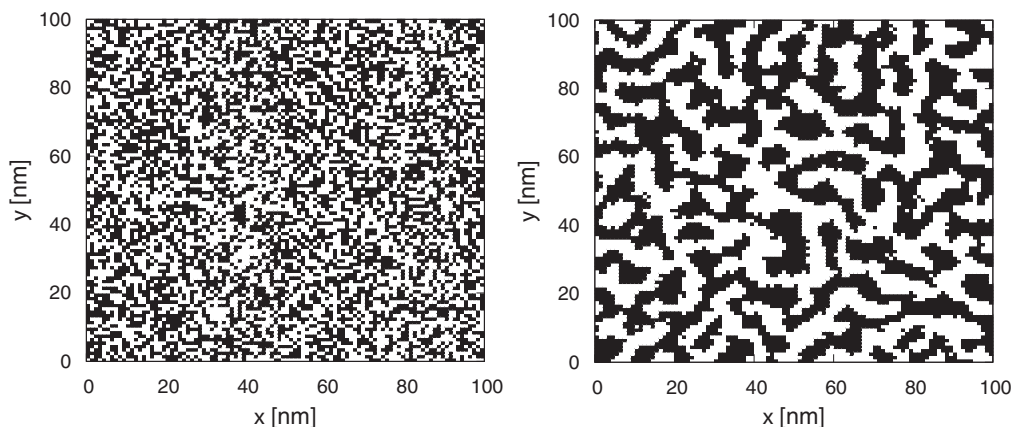


FIG. 1. Two-dimensional slice of the morphology with an equal amount of constituents (volume ratio $\alpha = 0.5$). The left plot illustrates a homogeneous mixture (domain size $b = 2$ nm) and the right plot a partially phase separated (domain size $b = 6$ nm).

Disordered organic materials, due to the large morphological disorder and the weak electronic coupling, have localized electronic states. The energetic distribution of these localized states in a one-phase system is usually assumed to be Gaussian.^{2,22} In this paper we will consider just electrons, with the extension to holes being straightforward. The probability density that a given site of a given phase has energy ε will be assumed to be given by

$$p(\varepsilon) = \frac{1}{\sqrt{2\pi}\sigma^2} \exp[-(\varepsilon - \varepsilon_L)^2/2\sigma^2], \quad (2)$$

where ε_L is the average energy of the given phase and σ is a measure of its energetic disorder. For the two-phase case this results in a bimodal Gaussian DOS,¹⁹ given by

$$g(\varepsilon; E_{\text{offset}}) = (1 - \alpha)p_1(\varepsilon) + \alpha p_2(\varepsilon), \quad (3)$$

where $E_{\text{offset}} \equiv \varepsilon_L^1 - \varepsilon_L^2$ is the energy offset (see schematic representation in Fig. 2). We will not consider here the possibility of the energies of the localized states to be correlated²³⁻²⁶ although this could be done.

The charge carrier mobility is calculated by solving numerically the steady-state Pauli master equation,

$$\sum_{j \neq i} [W_{i \rightarrow j} P_i (1 - P_j) - W_{j \rightarrow i} P_j (1 - P_i)] = 0, \quad (4)$$

where P_i is the probability that site i is occupied by a charge carrier, and $W_{i \rightarrow j}$ is the hopping rate from site i to site j . The $(1 - P_i)$ excludes, in a mean-field approximation,²⁷ the possibility of double occupancy. We ignored the Coulomb interaction between carriers in different sites since it was shown by Zhou *et al.*²⁸ that for low-carrier densities, such as the ones considered in this work, this effect is negligible.

The hopping rate is assumed to be of the Miller-Abrahams form:²⁹

$$W_{i \rightarrow j} = \begin{cases} w_0 \exp[-2\gamma R_{ij} - \Delta\varepsilon_{ji}/k_B T], & \Delta\varepsilon_{ji} \geq 0 \\ w_0 \exp[-2\gamma R_{ij}], & \Delta\varepsilon_{ji} < 0, \end{cases} \quad (5)$$

where w_0 is the intrinsic hopping rate, γ is the inverse localization length of the localized wave functions, assumed here be the same for both phases, $R_{ij} \equiv |\mathbf{R}_i - \mathbf{R}_j|$ is the distance between sites i and j , k_B is the Boltzmann constant,

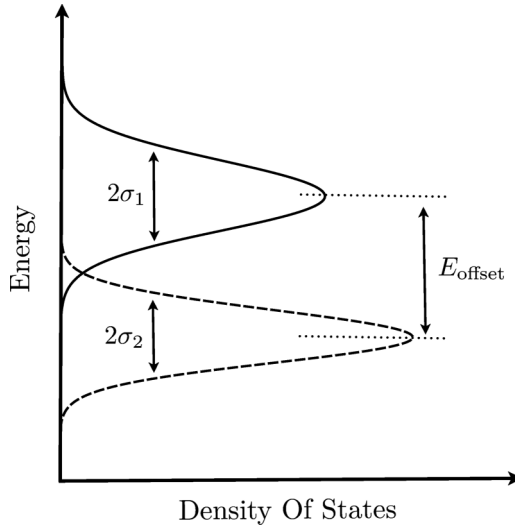


FIG. 2. Schematic bimodal Gaussian density of states diagram of the two-phase system. Each phase is characterized by a Gaussian distribution with width σ_1 (phase-1) and σ_2 (phase-2). The phase-2 average energy (the center of the Gaussian) is offset by E_{offset} with respect to the phase-1 average energy.

T is the temperature, and $\Delta\varepsilon_{ji} \equiv \varepsilon_j - \varepsilon_i - eFR_{ji}^x$, with ε_i and ε_j being the on-site energy of sites i and j , respectively. The term $-eFR_{ji}^x$ is the energy shift due to the electric field F , in the negative x direction, e is the elementary charge, and R_{ji}^x is the distance between sites j and i in the x direction. We consider hopping to a maximum distance of $\sqrt{3}a$, which takes into account 26 neighboring sites.

We solved Eq. (4) for the occupational probabilities P_i 's, using periodic boundary conditions by an iteration procedure originally proposed by Yu *et al.*³⁰ and later improved by Cottar *et al.*²⁷ Once the occupational probabilities are obtained, the charge-carrier mobility μ is calculated from

$$\mu = \frac{\sum_{i,j,j \neq i} W_{i \rightarrow j} P_i (1 - P_j) R_{ij}^x}{nFV}, \quad (6)$$

where $n = \langle P_i \rangle / a^3$ and V is the system volume. The lattice size is $N = 100^3$. Averages over a number of different disorder configurations and different morphologies (with fixed domain size and volume ratio) were taken until an accuracy better than 10% was obtained for μ .

Throughout the paper we fixed the inverse of localization length $\gamma = 10a^{-1}$, the carrier density $n = 10^{-6}a^{-3}$, the lattice constant $a = 1$ nm, the thermal energy $k_B T = 0.025$ eV (room temperature), and the intrinsic transition rate $w_0 \sim 4.8 \times 10^{20} \text{ s}^{-1}$, which leads to a maximum transition rate between nearest neighbor of the order of 10^{12} s^{-1} .^{2,31}

III. DOS DEPENDENCE

In this section we will focus on the zero electric field regime, $F \rightarrow 0$, and set the domain size $b = 6$ nm and the volume ratio $\alpha = 0.5$.

In Fig. 3 we show, in a semilog scale, the effect of the energetic disorder of the phase-2, σ_2 , on the mobility. We fixed $E_{\text{offset}} = 0$, and considered four different values of the energetic disorder of phase-1, σ_1 . It is clear that the

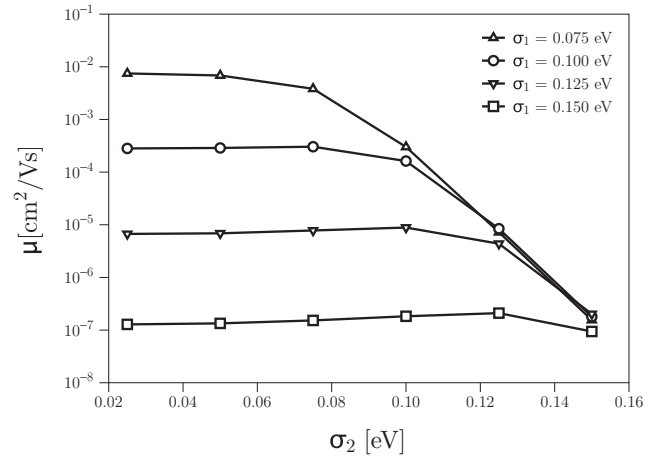


FIG. 3. Mobility as a function of the phase-2 energetic disorder σ_2 , for selected values of the phase-1 energetic disorder σ_1 . For all cases the domain size $b = 6$ nm, the volume ratio $\alpha = 0.5$, and the energy offset $E_{\text{offset}} = 0$.

mobility becomes independent of σ_2 when $\sigma_2 < \sigma_1$. This means that, when $E_{\text{offset}} = 0$, the mobility is controlled by the more disordered phase. This result can be explained as follows: In the low-carrier concentration regime, for the unimodal Gaussian DOS the majority of states that participate in the transport are states located around the transport level, $E_t = \varepsilon_L - \sigma^2/kT$, in the tail of the DOS.^{32,33} In the bimodal Gaussian DOS case, when $E_{\text{offset}} = 0$, these tail states belong mostly to the more disordered phase. So, if there is no energy offset between the two phases, the more ordered phase barely contributes to the transport.

In Fig. 4, we show, in a semilog scale, the effect of the energy offset E_{offset} on the mobility. We fixed $\sigma_1 = 0.1$ eV, and considered four different values of E_{offset} . This figure can be split in three different cases: (i) For $\sigma_2 < \sigma_1$ the mobility increases with the increase of E_{offset} . (ii) For $\sigma_2 \geq \sigma_1$ the opposite behavior happens; the mobility decreases with the increase of E_{offset} . (iii) Above a certain value ($E_{\text{offset}} \sim 0.3$ eV in that figure) the mobility becomes independent of E_{offset} .

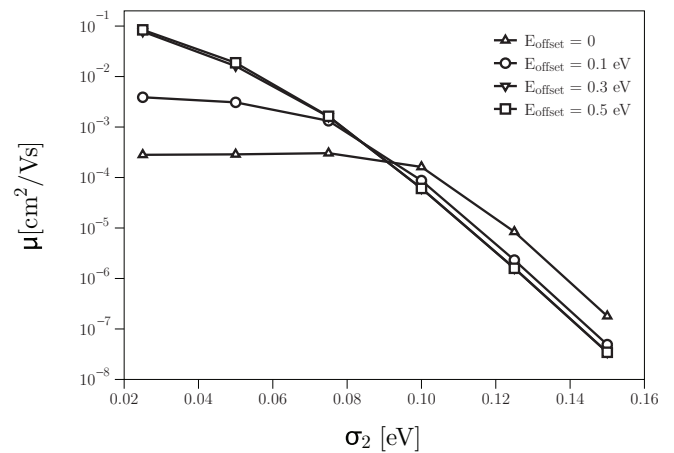


FIG. 4. Mobility as a function of the phase-2 energetic disorder σ_2 for the phase-1 energetic disorder fixed at $\sigma_1 = 0.1$ eV. For all cases the domain size $b = 6$ nm and the volume ratio $\alpha = 0.5$.

In case (i), when E_{offset} increases the tail states of the (more ordered) phase-2 get lower in energy and dominate the transport. Case (ii) follows the same trend of case (i) except that in this case the dominant phase-2 is less ordered, so that the larger the E_{offset} the smaller the mobility. Finally, in case (iii), when E_{offset} is larger than a threshold value, the transport goes entirely through phase-2 and the mobility dependence on σ_2 is characteristic of the particular topology of phase-2. Case (iii) is the typical case encountered in donor-acceptor mixtures, when E_{offset} between either LUMOs or HOMOs is “large enough” to confine electrons to the acceptor phase and holes to the donor phase. In the next section we will discuss more precisely this limiting case.

IV. MORPHOLOGY DEPENDENCE

In this section we will still focus on the low field regime but will now address the effect of the morphology of the two-phase mixture on the mobility. The volume ratio in the ranges $[0,0.2]$ and $[0.8,1.0]$ will not be considered here. In these ranges trapping and de-trapping effects become important and these are out of the scope of this paper. A good discussion about these two ranges for a random two-phase mixture can be found in Ref. 19.

A. Volume ratio dependence

In Fig. 5 we show, in a semilog scale, the effect of the volume ratio α (the fraction of phase-2 sites) on the mobility, normalized to the phase-1 mobility $\mu(\alpha = 0) = 2.8 \times 10^{-4} \text{ cm}^2/\text{Vs}$. We fixed $b = 6 \text{ nm}$, $\sigma_1 = \sigma_2 = 0.1 \text{ eV}$, and considered six different values of E_{offset} . $E_{\text{offset}} = 0$, represents a one-phase system and the mobility is not affected by α . For $E_{\text{offset}} > 0$, the mobility clearly decreases with increasing E_{offset} and decreasing α . This happens because in both cases the number of sites that participate in the transport (that takes place mainly in the less energetic phase-2) is reduced. The limiting case $E_{\text{offset}} \rightarrow \infty$, when the transport takes place only in phase-2, falls in the Koster model.¹⁶

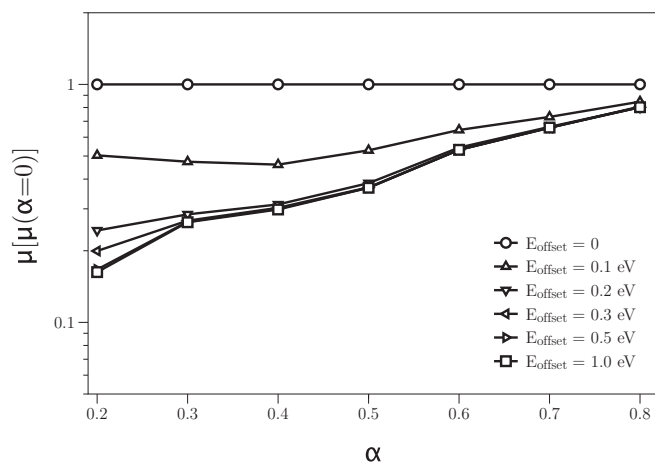


FIG. 5. Mobility as a function of the volume ratio α (the fraction of phase-2 sites) for selected values of the energy offset E_{offset} . Both phases are equally disordered, $\sigma_1 = \sigma_2 = 0.1 \text{ eV}$. For all cases the domain size $b = 6 \text{ nm}$. The mobility is normalized to the phase-1 mobility $\mu(\alpha = 0) = 2.8 \times 10^{-4} \text{ cm}^2/\text{Vs}$.

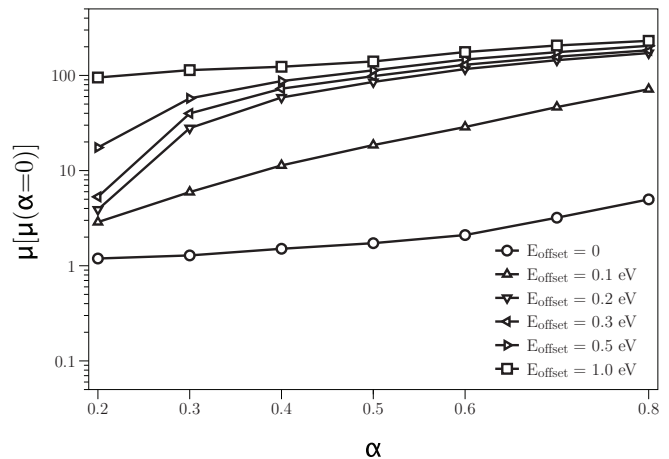


FIG. 6. Mobility as a function of the volume ratio α (the fraction of phase-2 sites) for selected values of the energy offset E_{offset} . Here the less energetic phase is more ordered ($\sigma_1 = 0.1 \text{ eV}$ and $\sigma_2 = 0.05 \text{ eV}$). For all cases the domain size $b = 6 \text{ nm}$. The mobility is normalized to the phase-1 mobility $\mu(\alpha = 0) = 2.8 \times 10^{-4} \text{ cm}^2/\text{Vs}$.

In Fig. 6 we show, in a semilog scale, the effect of the volume ratio α on the mobility, again normalized to the phase-1 mobility $\mu(\alpha = 0) = 2.8 \times 10^{-4} \text{ cm}^2/\text{Vs}$. We fixed $b = 6 \text{ nm}$, $\sigma_1 = 0.1 \text{ eV}$, and $\sigma_2 = 0.05 \text{ eV}$ (the less energetic phase is more ordered) and considered six different values of E_{offset} . In this case the mobility still decreases with decreasing α for the same reason seen in Fig. 5. But here, in contrast to Fig. 5, the mobility increases with increasing E_{offset} . This can be explained as follows: With increasing E_{offset} the transport gradually becomes more restricted to the phase with the lower energetic landscape, that is, phase-2. In Fig. 5, both phases had the same energetic disorder, so that the final result was just a reduction on the number of sites that contribute to the transport. But in Fig. 6 the phase with lower energy is more ordered, the restriction of the transport to this phase (due to an increase in E_{offset}) has a positive effect on the mobility that more than compensates for the negative effect associated with the reduction of the number of sites taking part in the transport.

Figure 6 suggests that in systems like amorphous-crystalline blends even small amounts of crystalline domains ($\sim 20\%$) can improve the mobility. The larger E_{offset} the larger this effect. Representative examples of this enhancement in organic materials can be found in Refs. 34 and 35.

B. Domain size and energy offset dependence

In Fig. 7 we show, in a semilog scale, the effect of the energy offset E_{offset} , and the domain size b on the mobility, again normalized to the phase-1 mobility $\mu(\alpha = 0) = 2.8 \times 10^{-4} \text{ cm}^2/\text{Vs}$. We fixed $\sigma_1 = \sigma_2 = 0.1 \text{ eV}$, $\alpha = 0.5$, and selected four different values of b . $E_{\text{offset}} = 0$ represents the one-phase case and the mobility is not affected by b . For $E_{\text{offset}} > 0$, this plot makes evident that the mobility is enhanced by increasing b . The domain size b has a direct impact on the channel network of each phase. As it increases the number of direct percolative paths from one electrode to the other increases, thereby increasing the mobility. For E_{offset} above

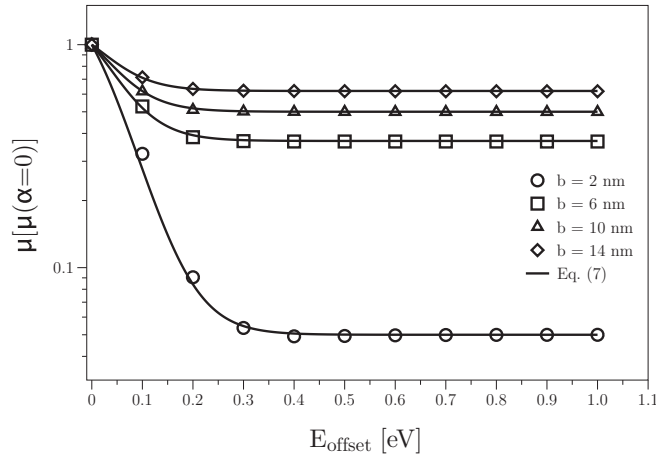


FIG. 7. Mobility as a function of the energy offset for selected values of the domain size b . For all cases the volume ratio $\alpha = 0.5$, and both phases are equally disordered, $\sigma_1 = \sigma_2 = 0.1$ eV. The mobility is normalized to the phase-1 mobility $\mu(\alpha = 0) = 2.8 \times 10^{-4}$ cm²/Vs.

0.3 eV the transport becomes entirely restricted to the less energetic phase-2 and the mobility no longer depends on E_{offset} .

For the case $\sigma_1 = \sigma_2 = 0.1$ eV, shown in Fig. 7, we obtained an analytical expression for the mobility as a function of the energy offset and parametric in b and σ_1 . The expression is given by

$$\mu(E_{\text{offset}}; b, \alpha, \sigma_1) = \mu_{\text{Pasveer}}(\sigma_1) \times f(E_{\text{offset}}; b, \alpha, \sigma_1), \quad (7)$$

where $\mu_{\text{Pasveer}}(\sigma_1)$ is the mobility at $E_{\text{offset}} = 0$, which coincides with the mobility obtained from Pasveer's model,¹² and

$$f(E_{\text{offset}}; b, \alpha, \sigma_1) = 1 - A(b, \alpha) \tanh(\sigma_1^{-1} E_{\text{offset}}), \quad (8)$$

with $A(b, \alpha)$ given in Table I for various values of α and b . Equations (7) and (8) are valid in the regime of low field and low-carrier density. Equation (8) holds for $E_{\text{offset}} \gg \sigma_1 (= \sigma_2)$, typical in BHJs solar cells ($E_{\text{offset}} > 0.5$ eV). In this limit Eq. (8) becomes $f(E_{\text{offset}}; b, \alpha) = 1 - A(b, \alpha)$.

It has been reported in the literature that (i) the electron-only and hole-only mobilities in donor-acceptor blends can be smaller than in the neat material counterpart³⁶ and (ii) thermal annealed blends have higher mobility than as cast.^{36,37} These two results can be understood using Eq. (7).

Clearly from Eq. (7) the neat material, $E_{\text{offset}} = 0$, has a higher mobility than the blend case, $E_{\text{offset}} \gg 0$. But the ratio between the two mobilities will depend on the domain size b ,

TABLE I. The fitting parameter $A(b, \alpha)$, used in Eq. (7), calculated for different values of the domain size b , and the volume ratio α . The smaller $A(b, \alpha)$ the higher the mobility.

$\alpha \backslash b$ (nm)	2	6	10	14
0.3	0.98	0.73	0.57	0.42
0.4	0.97	0.70	0.53	0.42
0.5	0.95	0.63	0.50	0.38
0.6	0.82	0.47	0.34	0.27
0.7	0.63	0.34	0.20	0.19

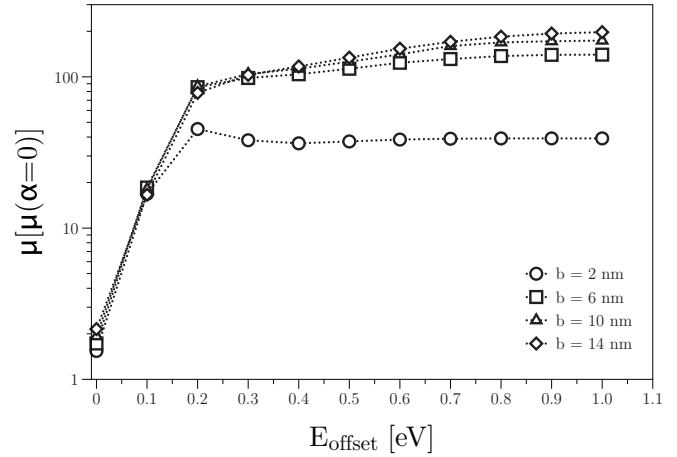


FIG. 8. Mobility as a function of the energy offset for selected values of the domain size b . For all cases the volume ratio $\alpha = 0.5$; the more energetic phase is less ordered than the less energetic phase ($\sigma_1 = 0.1$ eV and $\sigma_2 = 0.05$ eV). The mobility is normalized to the phase-1 mobility $\mu(\alpha = 0) = 2.8 \times 10^{-4}$ cm²/Vs.

and on the volume ratio α , used in the blend. Assuming that the thermal annealing process favors larger phase separation, hence larger domain sizes b , the mobility in the annealed blend will end up having larger mobility than the nonannealed one.

In Fig. 8 we continue to analyze the effect of the domain size on the mobility but, instead of assuming equally disordered phases as in Fig. 7, we take the less energetic phase as more ordered, $\sigma_1 = 0.1$ eV and $\sigma_2 = 0.05$ eV. This case attempts to model amorphous-crystalline mixtures, as seen in some conjugated polymers like P3HT³⁸ and PBTTT³⁹ using x-ray diffraction techniques. As seen in the $\sigma_1 = \sigma_2$ case, the larger the domain size the larger the mobility. However, as E_{offset} increases the mobility becomes larger (not smaller as in Fig. 7) than the mobility at $E_{\text{offset}} = 0$, because the transport becomes more restricted to the more ordered phase (same effect seen in Fig. 6). For E_{offset} above 0.2 eV the transport is exclusively through the less energetic phase and the mobility becomes independent of E_{offset} .

V. ELECTRIC FIELD DEPENDENCE

We have discussed so far the effect of disorder and morphology in the zero field regime. In this section we will discuss the influence of the electric field on the mobility in the two cases presented in the previous section: both phases equally disordered and the less energetic phase more ordered. We will assume here $b = 6$ nm and $\alpha = 0.5$.

In Fig. 9 we show, in a semilog scale, the effect of the electric field F on the mobility. We fixed $\sigma_1 = \sigma_2 = 0.1$ eV and considered six different values of E_{offset} . $E_{\text{offset}} = 0$ represents a one-phase system and, as mentioned before, coincides with Pasveer's model for the charge density used, $n = 10^{-6}$ a⁻³.¹² In this case the mobility increases monotonically with increasing F . For $E_{\text{offset}} > 0$, the mobility has a negative field dependence followed by a positive field dependence. The negative field dependence was discussed by Bäessler³ and Koster¹⁶ in the context of a single-phase system. The effect was explained

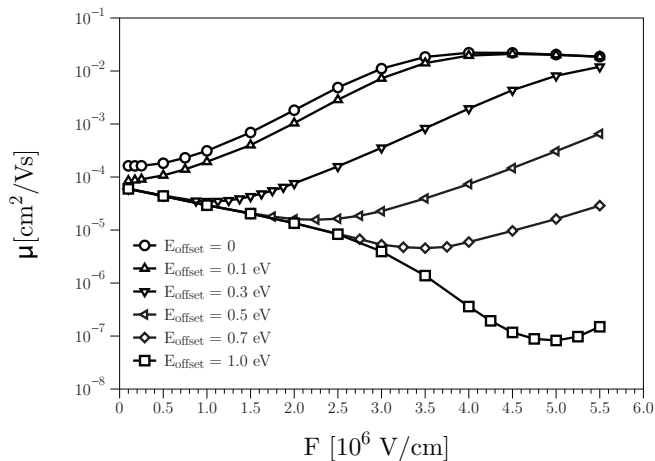


FIG. 9. Mobility as a function of the electric field for selected values of the energy offset E_{offset} . For all cases the domain size $b = 6$ nm, the volume ratio $\alpha = 0.5$, and both phases are equally disordered, $\sigma_1 = \sigma_2 = 0.1$ eV.

in terms of paths that go against the field that contribute to the mobility at very low fields but cease to contribute (hence decreasing the mobility) as the field increases. Above a certain F_{min} only paths that go mostly along the field contribute and the mobility along these paths increases with increasing F . What is displayed in Fig. 9 is a somewhat similar effect on a two-phase system. The $E_{\text{offset}} = 0$ curve corresponds to a single-phase system; F_{min} is located at very low fields and is barely visible in that figure. For $E_{\text{offset}} > \sigma_1 + \sigma_2$ ($=0.2$ eV in the case of Fig. 9) the carrier is entirely restricted to the less energetic phase-2 at low fields; the observed decrease of μ below F_{min} is the effect of the field in the transport through the channel network of phase-2. Above F_{min} the field can provide energy for the carrier to hop into the more energetic phase-1 (it is significant that $eF_{\text{min}}a$ is of the order of E_{offset}), and a number of paths that were forbidden at low fields become available, resulting in a mobility increase.

In Fig. 10 we show, in a semilog scale, the effect of the electric field F on the mobility, exactly like in Fig. 9, but

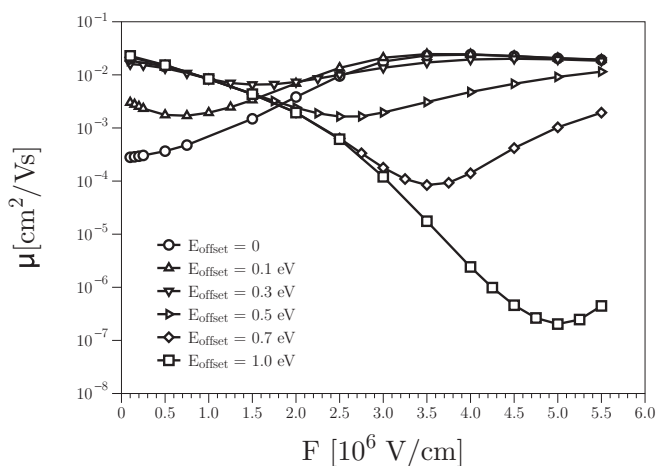


FIG. 10. Mobility as a function of the electric field for selected values of the energy offset E_{offset} . For all cases the domain size $b = 6$ nm and the volume ratio $\alpha = 0.5$; here the more energetic phase is less ordered, $\sigma_1 = 0.1$ eV and $\sigma_2 = 0.05$ eV

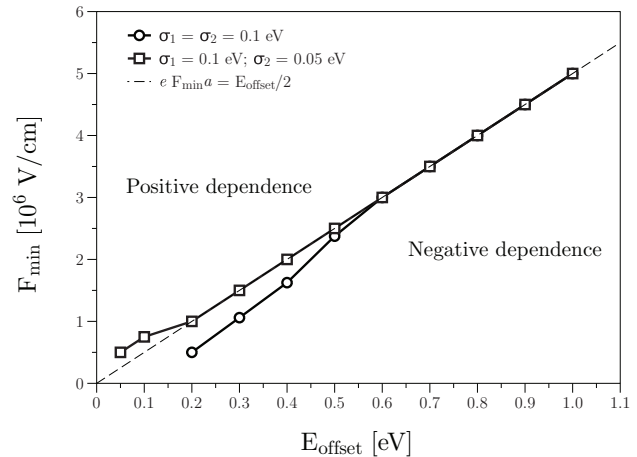


FIG. 11. The relation between the electric field at the transition between positive and negative field dependence F_{min} , with the energy offset E_{offset} , with the domain size $b = 6$ nm, the volume ratio $\alpha = 0.5$, and two different energetic disorder cases: (i) Circles, $\sigma_1 = \sigma_2 = 0.1$ eV and (ii) squares, $\sigma_1 = 0.1$ eV and $\sigma_2 = 0.05$ eV.

now we took the less energetic phase as more ordered ($\sigma_1 = 0.1$ eV and $\sigma_2 = 0.05$ eV). As in the $\sigma_1 = \sigma_2$ case of Fig. 9, a negative dependence followed by a positive dependence occurs. However, the general behavior of the curves in Fig. 10 differ from the corresponding ones in Fig. 9 at low fields (below 2×10^6 V/cm). In this low field range the mobility increases with E_{offset} and the field does not have a major effect. One is simply observing (as E_{offset} increases) the transport becoming restricted to the more ordered phase (hence the increase in μ). For higher fields (above 2×10^6 V/cm) the mobility displays the same ‘‘dip’’ seen in Fig. 9 and the explanation is the same: Below F_{min} the carrier is restricted to phase-2 and above F_{min} it gains access to the more energetic phase-1.

In Fig. 11 we plot the threshold electric field F_{min} of Figs. 9 and 10 against E_{offset} . In both cases we can see that F_{min} has an asymptotic dependence on E_{offset} given by $F_{\text{min}} = E_{\text{offset}}/2$. This supports the argument that F_{min} is the field value above which the carrier starts to penetrate in the more energetic phase.

VI. SUMMARY AND CONCLUSIONS

We have applied a three-dimensional Pauli master equation model with a bimodal Gaussian density of states to investigate the influence of morphology, disorder, and electric field on the charge carrier mobility of a two-phase system in the low-carrier density limit. At low electric fields we showed that the carrier mobility has a completely different behavior when compared to a single-phase system, depending on the energy offset parameter E_{offset} . In the limiting case $E_{\text{offset}} \rightarrow 0$, the mobility is controlled by the more disordered phase. The other limit, $E_{\text{offset}} \rightarrow \infty$, falls in the Koster model,¹⁶ when the transport becomes restricted to the less energetic phase. For intermediate values of E_{offset} , we have shown that even low amounts ($\sim 20\%$) of ordered domains can greatly enhance the mobility of a disordered material. This result is significant

for amorphous-crystalline mixtures. This enhancement is more significant if the ordered phase is distributed in large domains.

For the two cases considered in this paper, the two phases being equally disordered and the less energetic phase being more ordered, we have shown that the electric field dependence of the mobility shows a minimum at an electric field of the order of half the energy offset of the two phases. In practice, this finding can provide a rough idea in which regime (negative or positive mobility field dependence) a particular system, for instance, a donor-acceptor blend, will operate at a given electric field.

As for improvements we point out that we restricted ourselves to the low-carrier density limit; it is now necessary to go beyond this limit to see how the carrier density affects our results. It will also be important to investigate the carrier mobility at low temperatures and check if the controversial

$1/T^2$ dependence, found in one-phase systems,^{40,41} is also present in two-phase systems.

ACKNOWLEDGMENTS

The authors would like to thank F. Andrade, J. Love, M. Kuik and P. Zalar for their useful comments and suggestions. Furthermore, computational support from the Center for Scientific Computing at the CNSI and MRL, an NSF MRSEC (Grant No. DMR-1121053), and NSF Grant No. CNS-0960316, are acknowledged. The work was supported by CNPq (Brazil) fellowship (200974/2011-4) and the National Science Foundation (NSF) Division of Materials Research, NSF-SOLAR (Grant No. DMR-1035480). T.Q.N. thanks the Camille Dreyfus Teacher Scholar Award and the Alfred Sloan Research Fellowship program. G.L. thanks the support of NSF-PREM (Grant No. DMR-1205734).

*crisfisico@gmail.com

¹T. W. Kelley, P. F. Baude, C. Gerlach, D. E. Ender, D. Muires, M. A. Haase, D. E. Vogel, and S. D. Theiss, *Chem. Mater.* **16**, 4413 (2004).

²H. Bässler, *Phys. Status Solidi B* **107**, 9 (1981).

³H. Bässler, *Phys. Status Solidi B* **175**, 15 (1993).

⁴C. Adachi, M. A. Baldo, M. E. Thompson, and S. R. Forrest, *J. Appl. Phys.* **90**, 5048 (2001).

⁵J. Zaumseil and H. Sirringhaus, *Chem. Rev.* **107**, 1296 (2007).

⁶S. Baranovskii, I. Zvyagin, H. Cordes, S. Yamasaki, and P. Thomas, *J. Non-Cryst. Solids* **299–302**, 416 (2002).

⁷S. Baranovskii, I. Zvyagin, H. Cordes, S. Yamasaki, and P. Thomas, *Phys. Status Solidi B* **230**, 281 (2002).

⁸R. Schmechel, *Phys. Rev. B* **66**, 235206 (2002).

⁹V. Arkhipov, P. Heremans, E. V. Emilianova, G. J. Adriaenssens, and H. Bässler, *J. Phys.: Condens. Matter* **14**, 9899 (2002).

¹⁰S. Shaked, S. Tal, Y. Roichman, A. Razin, S. Xiao, Y. Eichen, and N. Tessler, *Adv. Mater.* **15**, 913 (2003).

¹¹Y. Roichman and N. Tessler, *Synth. Met.* **135–136**, 443 (2003).

¹²W. F. Pasveer, J. Cottaar, C. Tanase, R. Coehoorn, P. A. Bobbert, P. W. M. Blom, D. M. de Leeuw, and M. A. J. Michels, *Phys. Rev. Lett.* **94**, 206601 (2005).

¹³G. Yu, J. Gao, J. C. Hummelen, F. Wudl, and A. J. Heeger, *Science* **270**, 1789 (1995).

¹⁴P. Blom, V. Mihailetschi, L. J. A. Koster, and D. E. Markov, *Adv. Mater.* **19**, 1551 (2007).

¹⁵P. K. Watkins, A. B. Walker, and G. L. B. Verschoor, *Nano Lett.* **5**, 1814 (2005).

¹⁶L. J. A. Koster, *Phys. Rev. B* **81**, 205318 (2010).

¹⁷C. Deibel and V. Dyakonov, *Rep. Prog. Phys.* **73**, 096401 (2010).

¹⁸J. C. Blakesley and D. Neher, *Phys. Rev. B* **84**, 075210 (2011).

¹⁹Y. Y. Yimer, P. A. Bobbert, and R. Coehoorn, *J. Phys.: Condens. Matter* **20**, 335204 (2008).

²⁰H. T. Nicolai, M. M. Mandoc, and P. W. M. Blom, *Phys. Rev. B* **83**, 195204 (2011).

²¹D. H. Rothman and S. Zaleski, *Rev. Mod. Phys.* **66**, 1417 (1994).

²²E. A. Silinsh, *Phys. Status Solidi A* **3**, 817 (1970).

²³Y. N. Gartstein and E. M. Conwell, *Chem. Phys. Lett.* **245**, 351 (1995).

²⁴S. V. Novikov, D. H. Dunlap, V. M. Kenkre, P. E. Parris, and A. V. Vannikov, *Phys. Rev. Lett.* **81**, 4472 (1998).

²⁵J. A. Freire and C. Tonezer, *J. Chem. Phys.* **130**, 134901 (2009).

²⁶J. J. M. van der Holst, F. W. A. van Oost, R. Coehoorn, and P. A. Bobbert, *Phys. Rev. B* **83**, 085206 (2011).

²⁷J. Cottaar and P. A. Bobbert, *Phys. Rev. B* **74**, 115204 (2006).

²⁸J. Zhou, Y. C. Zhou, J. M. Zhao, C. Q. Wu, X. M. Ding, and X. Y. Hou, *Phys. Rev. B* **75**, 153201 (2007).

²⁹A. Miller and E. Abrahams, *Phys. Rev.* **120**, 745 (1960).

³⁰Z. G. Yu, D. L. Smith, A. Saxena, R. L. Martin, and A. R. Bishop, *Phys. Rev. Lett.* **84**, 721 (2000).

³¹J. L. Brédas, D. Beljonne, V. Coropceanu, and J. Cornil, *Chem. Rev.* **104**, 4971 (2004).

³²D. Monroe, *Phys. Rev. Lett.* **54**, 146 (1985).

³³V. I. Arkhipov, E. V. Emelianova, and G. J. Adriaenssens, *Phys. Rev. B* **64**, 125125 (2001).

³⁴D. P. McMahan, D. L. Cheung, L. Goris, J. Dacuña, A. Salleo, and A. Troisi, *J. Phys. Chem. C* **115**, 19386 (2011).

³⁵J. Rivnay, R. Steyrlleuthner, L. H. Jimison, A. Casadei, Z. Chen, M. F. Toney, A. Facchetti, D. Neher, and A. Salleo, *Macromolecules* **44**, 5246 (2011).

³⁶V. D. Mihailetschi, H. X. Xie, B. de Boer, L. J. A. Koster, and P. Blom, *Adv. Funct. Mater.* **16**, 699 (2006).

³⁷C. Groves, O. G. Reid, and D. S. Ginger, *Acc. Chem. Res.* **43**, 612 (2010).

³⁸S. Ko, E. T. Hoke, L. Pandey, S. Hong, R. Mondal, C. Risko, Y. Yi, R. Noriega, M. D. McGehee, J. L. Brédas, A. Salleo, and Z. Bao, *J. Am. Chem. Soc.* **134**, 5222 (2012).

³⁹S. Himmelberger, J. Dacuña, J. Rivnay, L. H. Jimison, T. McCarthy-Ward, M. Heeney, I. McCulloch, M. F. Toney, and A. Salleo, *Adv. Funct. Mater.* **23**, 2091 (2013).

⁴⁰N. I. Craciun, J. Wildeman, and P. W. M. Blom, *Phys. Rev. Lett.* **100**, 056601 (2008).

⁴¹R. Coehoorn, W. F. Pasveer, P. A. Bobbert, and M. A. J. Michels, *Phys. Rev. B* **72**, 155206 (2005).